COMSOL CONFERENCE 2025 AMSTERDAM

A COMSOL Multiphysics Approach to Simulate Graphene Defect Effects on the performance of Perovskite Solar Cell

Noor ul ain Ahmed[1], Monica La Mura [2] Vincenzo Tucci[1] , Patrizia Lamberti[1]

1. Department of Information and Electrical Engineering and Applied Mathematics, University of Salerno, 84084 Fisciano, (SA), Italy
2. Department of Industrial, Electronic, and Mechanical Engineering, Roma Tre University, Rome, Italy

Abstract

Perovskite solar cells (PSCs) are a promising photovoltaic technology, but their performance is limited by incomplete absorption of incident photons, particularly due to reflection at the transparent front electrode. Graphene, with its exceptional optical transparency and electrical conductivity, offers potential as a transparent electrode, yet its practical performance is affected by structural and chemical imperfections introduced during growth, deposition, and transfer process. In this work, COMSOL Multiphysics® is used to investigate how such imperfections influence the optical absorption of PSCs. A three-dimensional multilayer stack (glass/ITO/TiO_2/$MAPbI_3$/MoO_3/Ag) is modeled in the frequency domain using the Wave Optics Module, with graphene incorporated as a surface current boundary at the ITO/TiO_2 interface. The model reproduces the absorptance profile of a reference PSC and reveals that absorber thickness critically impacts the absorbance. Perovskite films thinner than 200 nm suffer reduced absorption, while thicker layers enhance light harvesting but exhibit Fabry–Pérot oscillations. Graphene introduces strong, tunable absorption in the THz regime via intraband transitions, whereas in the visible region its response is dominated by interband transitions, maintaining the universal ~2.3% absorption and high transparency. These results provide a modeling strategy to include graphene imperfections in device simulations and establish guidelines for the design of graphene-based transparent electrodes in next-generation PSCs.

Keywords: Perovskite solar cell, COMSOL Multiphysics, Optical simulation

Introduction

Perovskite solar cells (PSCs) have achieved a significant increase in power conversion efficiency (PCE), rising from early reports of 3–4% to confirmed single-junction efficiencies of over 26%[1]. PSCs are being considered as potential candidates for next-generation solar energy devices due to the rapid advancement of their performances, which are comparable to those of well-established photovoltaic technologies. While preserving low-cost solution-based processing, ongoing improvements in perovskite based solar devices continue to drive efficiency near theoretical limits [1]. However, reliability and stability remain significant issues, as perovskite materials degrade quickly and suffer energy losses due to defects and non-radiative recombination [3]. As a result, researchers are exploring new materials and interface engineering strategies to increase PSC stability and efficiency [4]. One of such strategies to enhance performance, is the integration of two dimensional (2D) materials, particularly graphene, into perovskite solar cell (PSC) architectures to increase the conductivity and overall efficiency of solar cells. Graphene, a single-atom-thick carbon sheet, exhibits exceptional mechanical strength (about 200 times that of steel), high electrical conductivity, and notable optical transparency (around 97.7%) [5].

However, in practice, large area graphene films typically contain defects and grain boundaries, which are characteristic of polycrystalline layers grown by chemical vapor deposition (CVD). These defects contribute to increased carrier scattering and resistivity, significantly lowering the electrical performance [6]. Experimental studies provide valuable insight into how defects in monolayer graphene affect solar cell performance [7], but such approach require significant efforts and it is time consuming.

On the other side, employing numerical simulations based on efficient methods, such as the finite element method (FEM) offer a robust framework to explore device physics under controlled conditions,

generating new insights while minimizing costly and complex experimental procedures [8].

In this study, COMSOL Multiphysics® is used to vary the chemical potential of graphene in the range of 0.1–0.6 eV to model (i) unintentional doping of monolayer graphene, arising from impurities at the metal–graphene interface that may induce a p-type shift, and (ii) intentional electrostatic gating of graphene. In this way, the effect of shifting the chemical potential on the optical response is assessed by examining the absorptance, showing how graphene's tunable properties enable absorption of incident radiation beyond the intrinsic spectrum of the perovskite absorber. Similarly, the effect on the electrical response is assessed by analysing the conductivity, demonstrating how graphene enhances charge transport when integrated as part of the hybrid transparent electrode.

Graphene-enriched Perovskite Solar Cell

The study adopts a conventional n–i–p structure consisting of glass/ITO as the transparent conducting substrate, a compact TiO_2 layer as the electron transport layer (ETL), a $CH_3NH_3PbI_3$ ($MAPbI_3$) perovskite absorber, MoO_3 as the hole transport layer (HTL), and Ag as the back electrode. A monolayer graphene sheet is introduced between the ITO and TiO_2 layers, functioning as part of a hybrid transparent electrode with ITO. In this configuration, graphene not only provides high optical transparency but also enhances the electrode's conductivity.

Modeling of the solar cell

The solar cell geometry was implemented in COMSOL Multiphysics® v6.3 using a 3D multilayer structure as shown in Figure 1. The model domain was defined as a rectangular block with a lateral size of 100 nm × 100 nm in the x–y plane and a height equal to the total thickness of the stacked layers (glass 40 nm, ITO 40 nm, graphene monolayer ~0.34 nm, TiO_2 ETL 10 nm, $MAPbI_3$ perovskite 400 nm, MoO_3 HTL 40 nm, and Ag electrode 40 nm)[9]. Layers were arranged along the z-axis, with the glass substrate at the top and the silver back contact at the bottom. Graphene was introduced between ITO and TiO_2, modeled as a conductive sheet, thus forming part of a hybrid transparent electrode. The geometry was constructed parametrically to allow variation of individual layer thicknesses during simulation sweeps. The optical properties of each material layer were defined using the refractive index from the built-in material library of COMSOL Multiphysics®.

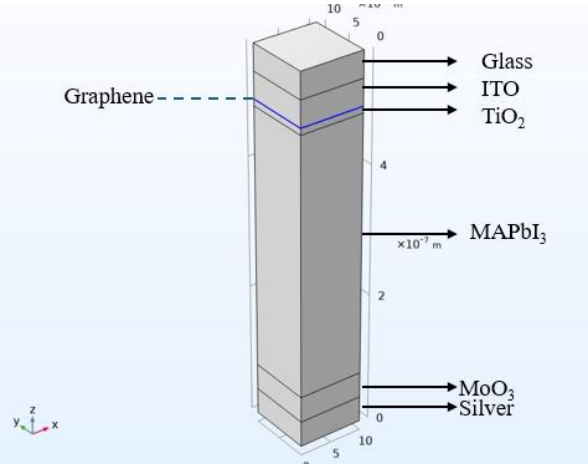

Figure 1. Geometry of the simulated perovskite solar cell stack constructed in COMSOL Multiphysics®.

Modeling of graphene

Graphene is atomically thin and typically modeled as a zero-thickness conductive sheet in COMSOL Multiphysics®, where the incident electromagnetic field induces a surface current defined by its frequency dependent conductivity [10]. In the finite element model, graphene was implemented as a surface current boundary condition at the ITO/TiO_2 interface. The surface current density follows

$$\underline{J} = \sigma\ \underline{E}$$

where σ is the complex surface conductivity described by the full Kubo formula, including both intraband and interband terms[11].

$$\sigma_{intra} = \frac{2\,k_B\,T\,e^2}{\pi\,\hbar^2}\ln\left(2\cosh\frac{E_f}{2\,k_B\,T}\right)\frac{-j}{\omega - j/\tau}$$

$$\sigma_{inter} = \frac{e^2}{4\,\hbar}\left[H\left(\frac{\omega}{2}\right) - j\frac{4\omega}{\pi}\right]\int_o^{\infty}\frac{H(\Omega) - H\left(\frac{\omega}{2}\right)}{\omega^2 - 4\Omega^2}\,d\Omega$$

where H is

$$H(\Omega) = sinh\left(\frac{\hbar\Omega}{k_B\,T}\right)/\left[\cosh\left(\frac{\hbar\Omega}{k_B\,T}\right) + cosh\left(\frac{E_f}{k_B\,T}\right)\right]$$

k_B is the Boltzmann constant, $\hbar$ is the reduced Planck constant, T is the absolute temperature, e is the electron charge, μ_c is graphene's chemical potential, and ω is the angular frequency

$$\omega = 2\pi f\,.$$

Introducing impurities or dopants injects charge carriers into graphene, shifting μ_c (i.e., moving the Fermi level up or down from the Dirac point [12]. In addition, applying an external gate voltage (i.e. electrostatic gating) also alters the chemical potential of graphene[13].In practice, researchers tune μ_c to represent how defects or chemical dopants alter graphene's electronic structure. An increase in p-

type carrier concentration reflects in a higher μ_c , that increases the conductivity of graphene and the resulting built-in electric field [10]. The chemical potential strongly affects the optical properties of graphene by modifying interband transitions. In undoped graphene, photons with sufficient energy can promote electrons from the valence to the conduction band, resulting in broadband absorption. When the Fermi level is shifted by doping or gating, however, many of the conduction-band states near the Dirac point become occupied. Following the Pauli exclusion principle, electrons in the valence band cannot be excited to these occupied states anymore and interband transitions are forbidden. This influence does not allow the photons to be absorbed with energy less than approximately twice the Fermi level (2 μ_c). As a result, increasing the chemical potential reduces low-energy absorption, making graphene more transparent in that spectral range[14]. n this way, the effect of defects on the conductivity and transparency of graphene can be captured in graphene based PSCs, which is essential to maximize the performances of solar cells.

Simulation setup

The Electromagnetic Waves, Frequency Domain (EWFD) interface in COMSOL Multiphysics® is applied to study the optical properties of a solar cell. The stack is excited from the glass/ITO side with a periodic port at normal incidence. Floquet periodic boundaries are set on the lateral faces (x–y) of the geometry to represent an infinitely extended planar device. The output port is applied at the bottom of the solar cell below the Ag layer. The model was discretized using a free tetrahedral mesh along the layered geometry to ensure accurate field resolution at each interface. The complete mesh consisted of 6374 domain elements, 1570 boundary elements, and 228 edge elements (Figure 2). The optical response was then solved in the frequency domain over the range 0.1–800 THz using the Electromagnetic Waves, Frequency Domain (EWFD) interface in COMSOL Multiphysics®. The parametric sweep is carried out for two different parameters, the perovskite absorber layer $MAPbI_3$ variation from 150-500nm to study the effect on the absorbance of solar cell and µc sweep from 0.1-0.6 eV to study the effect on absorbance, transparency and conductivity of graphene electrode.

Theory

The propagation of light through the perovskite solar cell stack is governed by Maxwell's equations in electromagnetic waves, frequency domain (ewfd) physics.

$$\nabla \times \mu_r^{-1}(\nabla \times E) - k_0^2 (\varepsilon_r - \frac{j\sigma}{\omega\varepsilon_0}) E = 0$$

Solver assumes.

$$\sigma = 0,$$
$$\mu_r = 1$$

which simplifies Maxwell's equation to

$$\nabla \times (\nabla \times E) - k_0^2 \varepsilon_r E = 0$$

In COMSOL's Wave Optics Module, materials are defined by their refractive index n and extinction coefficient k, which are internally converted into the complex permittivity [15].

$$\varepsilon_r = (n - jk)^2 ,$$

$$k_o = \frac{\omega}{c_0}$$

The geometry of the device is discretized into a fine mesh, allowing the solver to compute the Maxwell equation throughout the structure. The optical properties of each material, characterized by the refractive index (n) and the extinction coefficient (k), determine how light is transmitted, refracted, or absorbed. This framework enables incident light to interact with all layers of the device, quantifying absorption within the device and assessing how the electrical properties of graphene are tuned through chemical potential, influencing overall performance. Essentially, light enters from the top, and the physics interface resolves its propagation using the mesh, material data, and boundary conditions.

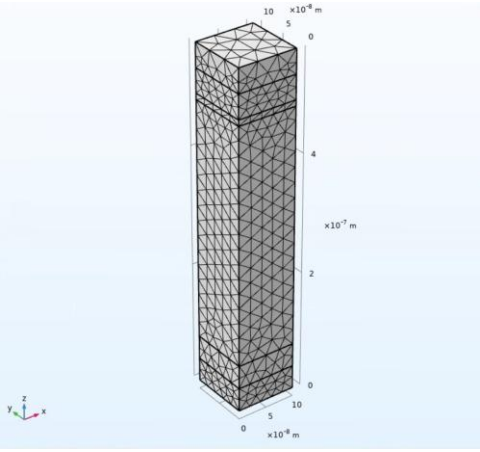

Figure 2. Finite element mesh of the perovskite solar cell model

Simulation Results

Effect of absorber layer thickness

The optical response of $CH_3NH_3PbI_3$ ($MAPbI_3$) perovskite layers with varying thicknesses (150–450 nm) was investigated using the Electromagnetic Waves, Frequency Domain (EWFD) interface in COMSOL Multiphysics. As shown in Figure 3, all

simulated structures exhibit high absorptance (>95%) in the 380–520 nm spectral range. For the thinnest layer (150 nm), a pronounced decline in absorptance is observed beyond 550 nm. In contrast, increasing the thickness to 250, 350, and 450 nm results in enhanced long wavelength absorption. However, the absorptance spectra of thicker films display distinct oscillatory features. These features arise from Fabry–Pérot interference, a consequence of multiple internal reflections within the PSC. The layered structure effectively behaves as an optical cavity, promoting standing wave formation and leading to thickness-dependent spectral modulation. This interference induced oscillations become more pronounced as the thickness increases, particularly in the 450 nm configuration. This behavior aligns with [16], where reduced device performance in sub-200 nm perovskite layers was attributed to limited absorption at longer wavelengths.

Effect of graphene

The effect of graphene chemical potential (μ_c) on optical absorption was analyzed across the 0–800 THz frequency range using the Electromagnetic Waves, Frequency Domain interface in COMSOL Multiphysics. As shown in Figure 4, the presence of a monolayer graphene sheet significantly enhances absorption in the low-frequency regime (<10 THz), where the structure without graphene exhibits negligible response (red curve). At very low frequencies (<1 THz), the highest peak absorptance (~0.97) is obtained for μ_c = 0.3 eV, indicating an optimal plasmonic coupling at this value. However, when considering the full frequency range (0–10 THz), the structure with μ_c = 0.6 eV consistently maintains higher absorptance. An enhancement in absorptance is observed as μ_c increases from 0.1 eV to 0.6 eV, confirming stronger coupling to plasmonic modes at higher doping levels [17].

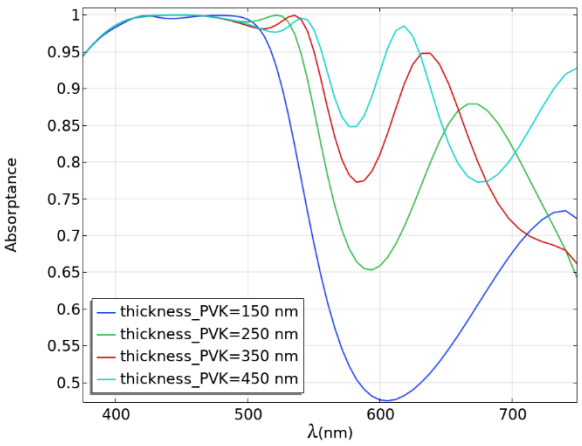

Figure 3. Optical absorptance as a function of thickness of absorber layer

The graphene induced absorption enhancement is frequency dependent and diminishes at higher frequencies (far-IR to visible range). As the frequency increases into the mid-infrared (tens to hundreds of THz) and beyond, the absorptance spectrum for different μ_c begins to converge (Figure 5). In this high-frequency regime, the presence of graphene makes little difference as all curves show similar interference, meaning the graphene's absorptive contribution becomes negligible relative to the overall response.

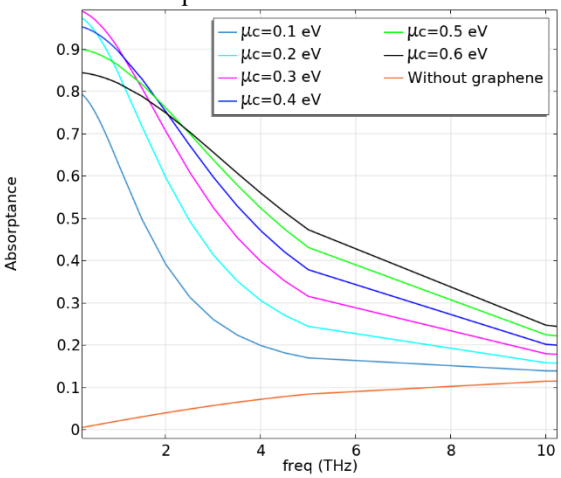

Figure 4. Absorptance spectra of the solar cell with and without graphene for different chemical potential (0-10 THz)

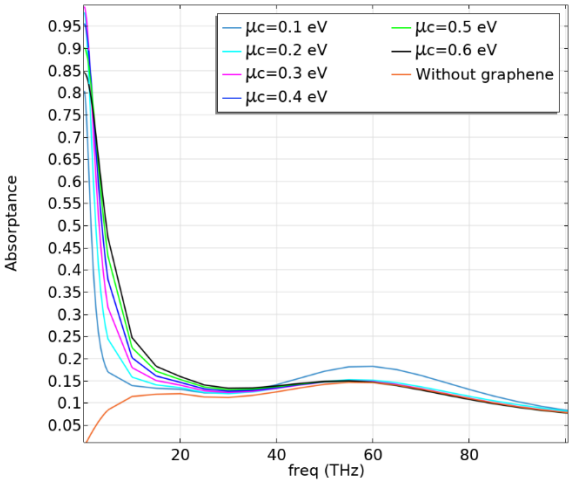

Figure 5. Absorptance spectra of the solar cell with and without graphene for different chemical potential (0-100 THz)

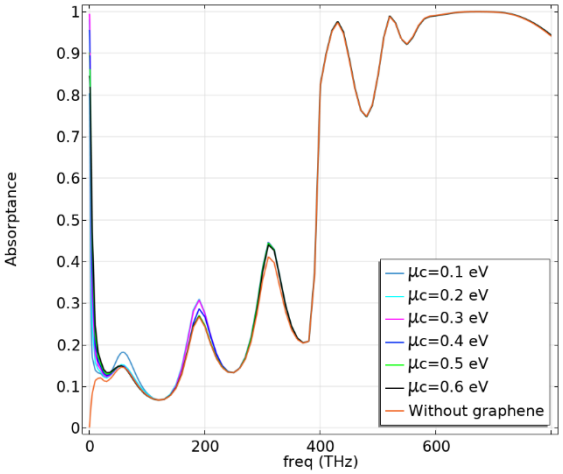

Figure 6. Absorptance spectra of the solar cell with and without graphene for different chemical potential (0-800 THz)

There are a couple of reasons for this. First, graphene's plasmonic response is strongest in the THz to mid-IR as doped graphene exhibits a pronounced Drude-like absorption peak in this low-frequency range, due to the high density of mobile charge carriers available for intraband transitions. At frequencies approaching visible, the photon energy exceeds twice the Fermi energy for these doping levels, damping out intraband plasmon resonances (graphene is almost transparent with its universal 2.3% absorption in the visible region [18]).

At higher frequencies, graphene's absorption is normally governed by interband transitions (electron transitions between valence and conduction bands). Undoped graphene displays a constant ~2.3% absorption per monolayer across the visible spectrum from such interband processes. When graphene is doped (with chemical potential $\mu_c \approx 0.1$–0.6 eV), the Fermi level shift causes Pauli blocking of interband transitions for photon energies below ~2 μc. As a result, doped graphene shows strong absorptance at THz frequencies (dominated by intraband transitions) but much weaker absorption in the mid-IR and higher-frequency ranges [19]. The cell absorption is not impaired by graphene impurities in visible range (Figure 6) makes it ideal transparent electrode for solar cells.

Figure 7 presents the full optical conductivity of monolayer graphene (from the Kubo formalism including both interband and intraband contributions) for various chemical potentials (μc = 0.1–0.6 eV). Across the visible spectrum, the conductivity stays nearly constant at ~6×10^{-5} S, with only a slight decline as the wavelength increases. Notably, the weak dependence on μc indicates that interband transitions dominate the response in this spectral region, while intraband contributions are negligible. This behavior corresponds to graphene's well-known universal optical conductivity, yielding an absorbance of about 2.3% per monolayer [20]. Such a universal absorbance has been experimentally observed by arising from the fundamental fine structure constant and the Dirac nature of graphene's electrons[21]. The small reduction in conductivity seen at higher μc is attributed to Pauli blocking, whereby increased Fermi level (due to doping) gradually suppresses interband transitions at longer wavelengths [22].

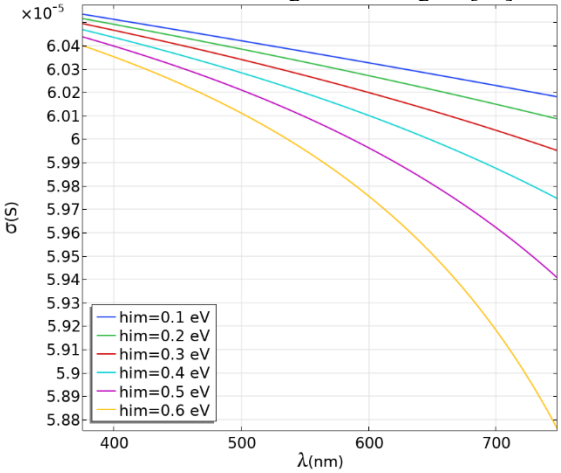

Figure7.Graphene's full conductivity (Intra+interband) as a function of its chemical potential

Figure 8 shows the intraband optical conductivity of graphene for different chemical potentials. The conductivity increases both with wavelength and μc, reflecting the Drude-like response of free carriers.

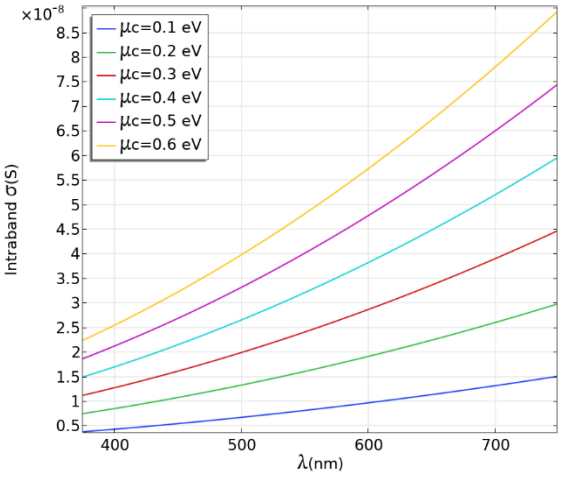

Figure 8. Graphene's Intraband conductivity as a function of its chemical potential

This trend explains the enhanced absorption observed in the THz regime, as μc increases, more carriers contribute to intraband transitions, leading to stronger plasmonic absorption peaks [23]. In contrast, at visible frequencies the intraband

contribution is negligible, and absorption is governed by the universal interband conductivity, confirming that graphene remains transparent in this region.

Conclusions

This work highlights the effect of absorber thickness and graphene conductivity on the performance of perovskite solar cell. Perovskite films thinner than 200 nm exhibit insufficient absorption in the long-wavelength region, while thicker layers (>250 nm) improve light harvesting but display Fabry–Perot oscillations. Incorporating a graphene monolayer introduces tunable absorption in the THz regime through intraband transitions that strengthen with the increase in chemical potential, while in the visible region, response is dominated by interband transitions, yielding the universal ~2.3% absorption and high transparency. These results confirm that graphene can act simultaneously as a transparent electrode in the visible and as a tunable plasmonic absorber at lower frequencies, underlining its suitability for advanced photovoltaic and optoelectronic applications.

Acknowledgements

EU NRRP NextGenerationEU (UPWARD CUP E53D23014490001, Decree 1383/2023), RESTART partnership (PE00000001), EU Horizon Europe MSCA (FLORIN GA n° 101086142).

References

[1] F. Ma, Y. Zhao, Z. Qu, and J. You, 'Developments of Highly Efficient Perovskite Solar Cells', *Accounts of Materials Research*, vol. 4, no. 8, pp. 716–725, 2023, doi: 10.1021/accountsmr.3c00068.

[2] C. Yang *et al.*, 'Achievements, challenges, and future prospects for industrialization of perovskite solar cells', *Light, science & applications*, vol. 13, p. 227, Sep. 2024, doi: 10.1038/s41377-024-01461-x.

[3] E. Danladi *et al.*, 'Defect and doping concentration study with series and shunt resistance influence on graphene modified perovskite solar cell: A numerical investigation in SCAPS-1D framework', *JOURNAL OF THE INDIAN CHEMICAL SOCIETY*, vol. 100, no. 5, May 2023, doi: 10.1016/j.jics.2023.101001.

[4] G. G. Njema, J. K. Kibet, and S. M. Ngari, 'A review of interface engineering characteristics for high performance perovskite solar cells', *Measurement: Energy*, vol. 2, p. 100005, 2024, doi: https://doi.org/10.1016/j.meaene.2024.100005.

[5] Z. al and A. Rehman, 'Recent progress in graphene incorporated solar cell devices', *Solar Energy*, vol. 169, pp. 634–647, Jul. 2018, doi: 10.1016/j.solener.2018.04.0419898.

[6] M. Bhatt, H. Kim, and G. Kim, 'Various defects in graphene: a review', *RSC Advances*, vol. 12, pp. 21520–21547, Aug. 2022, doi: 10.1039/D2RA01436J.

[7] E. Ros *et al.*, 'Impact of Graphene Monolayer on the Performance of Non-Conventional Silicon Heterojunction Solar Cells with MoOx Hole-Selective Contact', *Materials*, vol. 16, no. 3, 2023, doi: 10.3390/ma16031223.

[8] S. Zandi and M. Razaghi, 'Finite element simulation of perovskite solar cell: A study on efficiency improvement based on structural and material modification', *Solar Energy*, vol. 179, pp. 298–306, 2019, doi: https://doi.org/10.1016/j.solener.2018.12.032.

[9] L. Yue, B. Yan, M. Attridge, and Z. Wang, 'Light absorption in perovskite solar cell: Fundamentals and plasmonic enhancement of infrared band absorption', *Solar Energy*, vol. 124, pp. 143–152, 2016, doi: https://doi.org/10.1016/j.solener.2015.11.028.

[10] M. La Mura, P. Lamberti, and V. Tucci, 'Simulation of Graphene-based Materials and Devices for Sub-Terahertz Applications', Oct. 2023, pp. 901–905. doi: 10.1109/NMDC57951.2023.10343897.

[11] K. Ziegler, A. Hill, and A. Sinner, 'Electronic Transport and Optical Properties of Graphene', in *Graphene Optoelectronics*, John Wiley & Sons, Ltd, 2014, pp. 1–16. doi: https://doi.org/10.1002/9783527677788.ch1.

[12] S. Behura, C. Wang, Y. Wen, and V. Berry, 'Graphene–Semiconductor Heterojunction Sheds Light on Emerging Photovoltaics', *Nature Photonics*, vol. 13, Mar. 2019, doi: 10.1038/s41566-019-0391-9.

[13] G. Abbas *et al.*, 'Electrostatic Gating of Monolayer Graphene by Concentrated Aqueous Electrolytes', *The Journal of Physical Chemistry Letters*, vol. 14, no. 18, pp. 4281–4288, 2023, doi: 10.1021/acs.jpclett.3c00814.

[14] S. Adhikari *et al.*, 'Determining the Fermi level by absorption quenching of monolayer graphene by charge transfer doping', *Nanoscale*, vol. 8, no. 44, pp. 18710–18717, 2016, doi: 10.1039/C6NR05635K.

[15] Walter Frei, 'Modeling of Materials in Wave Electromagnetics Problems'. [Online]. Available: https://www.comsol.com/blogs/modeling-of-materials-in-wave-electromagnetics-problems

[16] L.-C. Chen, J.-C. Chen, C. Cheng-Chiang, and C.-G. Wu, 'Fabrication and Properties of High-

Efficiency Perovskite/PCBM Organic Solar Cells', *Nanoscale research letters*, vol. 10, p. 1020, Dec. 2015, doi: 10.1186/s11671-015-1020-2.

[17] M. Kim, T.-T. Kim, C. Kang, S. Kim, and C.-S. Kee, 'Highly efficient graphene terahertz modulator with tunable electromagnetically induced transparency-like transmission', *Scientific Reports*, vol. 13, Apr. 2023, doi: 10.1038/s41598-023-34020-2.

[18] T. Stauber, D. Noriega-Pérez, and J. Schliemann, 'Universal absorption of two-dimensional systems', *Phys. Rev. B*, vol. 91, no. 11, p. 115407, Mar. 2015, doi: 10.1103/PhysRevB.91.115407.

[19] T. Low and P. Avouris, 'Graphene Plasmonics for Terahertz to Mid-Infrared Applications', *ACS nano*, vol. 8, Jan. 2014, doi: 10.1021/nn406627u.

[20] K. F. Mak, M. Y. Sfeir, Y. Wu, C. H. Lui, J. A. Misewich, and T. F. Heinz, 'Measurement of the Optical Conductivity of Graphene', *Phys. Rev. Lett.*, vol. 101, no. 19, p. 196405, Nov. 2008, doi: 10.1103/PhysRevLett.101.196405.

[21] R. Raveendran-Nair *et al.*, 'Fine Structure Constant Defines Visual Transparency of Graphene', *Science (New York, N.Y.)*, vol. 320, p. 1308, Jul. 2008, doi: 10.1126/science.1156965.

[22] K. Mak, L. Ju, F. Wang, and T. Heinz, 'Optical spectroscopy of graphene: From the far infrared to the ultraviolet', *Solid State Communications*, vol. 152, pp. 1341–1349, Aug. 2012, doi: 10.1016/j.ssc.2012.04.064.

[23] P. Kumar, M. Silhavik, M. Parida, H. Nemec, J. Cervenka, and P. Kuzel, 'Terahertz Charge Transport Dynamics in 3D Graphene Networks with Localization and Band Regimes', *Nanoscale Advances*, vol. 5, May 2023, doi: 10.1039/D2NA00844K.